



Synthesis of Graphene from Lignin for Electrode Battery Applications.

Vorapas Hensawang^{*1,2}, Pornlada Daorattanachai¹, Navadol Laosiripojana¹,
Jakkapop Phanthasri², Saran Youngjan², and Pongtanawat Khemthong²

^{*}Corresponding author, E-mail: vorapas.hens@kmutt.ac.th

¹ The Joint Graduate School of Energy and Environment,
King Mongkut's University of Technology Thonburi, Thailand

² National Nanotechnology Center, National Science and Technology Development Agency,
Pathumthani 12120, Thailand

Abstract

Lignin obtained from the sugar industry is a potential feedstock for upgrading to produce value added chemicals. In this study, lignin-based graphene derived from extracted bagasse lignin samples was successfully synthesized by adding tetrahydrofuran as a modifier and metal nitrate salts (i.e., Ni and Fe) as catalysts in the pretreatment step to prepare metal-lignin precursors. Then, the metal-lignin precursors were heated via pyrolysis and exfoliated steps to obtain synthesized graphene. To identify important factors that control graphene synthesis, the effects of types of lignin, types of catalysts (metal nitrate salts), catalyst: lignin ratios, and holding time during pyrolysis were investigated. Moreover, the morphological and electrochemical properties of the prepared graphene were also measured to evaluate the possibilities of lignin-based graphene for anode materials in lithium-ion batteries. The experimental results revealed that at a current rate of 100 mA g⁻¹, the synthesized graphene used in the lithium-ion battery anode demonstrates a good specific capacity of 532 mA g⁻¹, which is 1.4 times higher than that of commercial graphite. The synthesized graphene also demonstrated high performance, with a coulombic efficiency of 99% after testing up to 300th cycles at a current density of 1 A g⁻¹.

Keywords: Bagasse Lignin, Graphene, Pyrolysis, Battery Applications

1. Introduction

In Thailand, the sugar industry has the capacity to produce 30 million tons of bagasse per year, or around 7.5 million tons of available lignin. Currently, sugarcane bagasse is used in factory cogeneration operations, with the surplus sold to community electricity plants (Liengprayoon, et al., 2019). To make better use of this agricultural by-product, it was proposed to separate and use lignin to manufacture higher-value goods before returning the dignified bagasse for energy production. Also, lignin has abundant functional groups, such as hydroxyl, benzyl, methoxyl, ether, and carboxyl, resulting in its amphiphilic nature. Hydroxyl is the most important functional group for lignin modifications, including alkylation, esterification, phenolation, and hydroxypropylation (Zhu, et al., 2020). However, lignin is a by-product from current pulping and bioethanol procedures, and when it can be used as a substitute carbon source for developing high-value carbon-based nanomaterials, that would encourage lignin's continued application. Making valuable carbon-based nanostructures like graphene from inexpensive lignin is essential. Significant efforts have focused on utilizing waste lignin as a component in polymer matrices for high-performance composite applications (Zhao, et al., 2020).

One kind of two-dimensional substance made of carbon monolayers with a sp² structure is called graphene. Graphene continued to gain substantial interest and application due to its unique characteristics,
[584]



such as its high theoretical surface area, exceptional thermal conductivity, and enhanced Young's modulus (Lee, Wei, Kysar, et al., 2008); (Zhu, et al., 2020). Various lignin forms can be used to synthesize graphene, including kraft lignin (Liu, et al., 2017), sodium lignosulfonate (Mandlekar, et al., 2018), and lignin that has been developed into nano-lignin (Dong, et al., 2020). Numerous synthesis techniques exist as well, including carbonization (Dong, et al., 2020), pyrolysis (Zhao, et al., 2020), photon etching, and catalyzed doping (Zhao, Tan, Zhang, & Liu, 2010). However, the application of graphene generated from lignin in energy storage devices is still relatively new (Kai, et al., 2016) (Liu, et al., 2021). The widespread use of lignin is a potentially efficient strategy to reduce environmental pollution. With the same logic, the use of electric vehicles (EVs) could positively impact the environment as they emit fewer greenhouse gases and air pollutants compared with conventional fuel-based vehicles (Jung, et al., 2022).

In this study, synthesized graphene from bagasse lignin as a solid carbon source for anode materials in lithium-ion batteries could positively affect the properties of the resulting materials. The study also investigates the variables that affect the synthesis and arrangement of graphene layers, and examines metal additives and holding times during the pyrolysis process. According to the synthesized graphene from lignin, it has morphology and electrochemical properties like commercial graphene. The study also evaluates graphene using lignin as the electrode material for batteries and finds it to be a promising alternative for electrochemical testing.

2. Objectives

- 1) To synthesize lignin-based graphene derived from extracted bagasse lignin
- 2) To characterize the physiochemical properties of synthesized graphene
- 3) To apply lignin-based graphene for lithium-ion battery anodes

3. Materials and Methods

3.1 Materials

Ethanol and hydrochloric acid (37%) were purchased from RCL Labscan Limited. Sulfuric acid (95-97%) was purchased from Merck KGaA. Tetrahydrofuran (THF, 99%) was purchased from Daejung Chemical and Metal. Iron (III) nitrate nonahydrate and nickel (II) nitrate hexahydrate were used as metal additives to compare synthesized graphene.

Several types of lignin were used as carbon sources in this study. Commercial organosolv lignin (CL) supplied by Chemical Point UG was used as a carbon source to prepare catalysts and biobased graphene. The lignin samples extracted from sugarcane bagasse were kindly provided by Thai Roong Ruang Sugar Group (Phetchabun, Thailand) and Mitr Phol Sugar Corporation., Ltd., (Chaiyaphum, Thailand).

3.2 Methods

3.2.1 Organosolv lignin preparation

3.2.1.1 Biomass preparation

Biomass was milled using a cutting mill and sieved to a size of <2 mm (Retsch model SM 2000). The biomass samples will be dried overnight at 60 °C.

3.2.1.2 Organosolv pretreatment

Organosolv pretreatment was carried out in the 2 L Parr reactor. The solvent was prepared by using 1 L of analytical-grade ethanol at a concentration of 70 % v/v. The sulfuric acid was used as a catalyst with 1% wt/v of biomass. A 100 g of prepared sugarcane bagasse was added to the prepared solvent with a 10% solid loading. The reaction was performed using nitrogen gas at 150 rpm and 180 °C for 60 minutes, with an initial pressure of 20 bar. The reaction was promptly stopped after the organosolv treatment by cooling it for 15 minutes in cool water. The liquid component of the slurry was separated from the solid part by filtering it

[585]



through Whatman No. 4 paper. Subsequently, the resulting liquid fraction was treated with three liters of water to precipitate the black liquor. The precipitated lignin was recovered by filtration through a filter paper, Whatman No.4, and then dried at room temperature for one day before use (Pongchaiphol, et al., 2022).

3.2.2 Synthesis of graphene

3.2.2.1 Preparation of a metal-lignin precursor with two different metal additives

At room temperature, a beaker was filled with 3.0 g of extracted lignin, various weight ratios of metal additives (metal/lignin 1:1, 1:2.5, and 1:3), 3 mL THF, and 50 mL deionized water. The solution was consistently stirred and transferred to a round-bottomed flask. The beaker was rinsed twice with 5 ml of deionized water before transferring the solution to the round bottom flask. The round bottom flask was placed in a water bath at 80 °C for 8 hours before being transferred to a drying oven at 110 °C overnight to produce a metal-lignin precursor (Zhao, et al., 2020).

3.2.2.2 Synthesis of graphene via pyrolysis

The porcelain sample boat and the metal-lignin precursor were placed inside the horizontal furnace. The tubular furnace was flowed with nitrogen gas at a rate of 100 ml/min. It was then heated to 180 °C at a rate of 5 °C/min, and it was kept there for 1 h. Subsequently, the temperature within the tubular furnace was continuously raised to 900°C at a rate of 5 °C/min. It was then held at that temperature for varying periods of time (120, 180, and 240 minutes) before being cooled to room temperature.

3.2.2.3 Exfoliation of graphene

The samples on the porcelain sample boat were collected and washed with 1 mol/L diluted hydrochloric acid (est. 40 mL) until there were no bubbles and the supernatant was clear. The solution was placed at room temperature for 24 hours. Following, the solution was kept in a water bath at 80 °C for 3 hours, cooled to room temperature, and ultrasonic treated for 2 hours. The samples were filtrated through a filter paper called Whatman No.1 and dried in an oven at 110 °C overnight to obtain the graphene. The synthesized graphene was given the designation G-X-M- [example]. Graphene was abbreviated as G, lignin sources were marked by X, and M were the types of metal additives. Specifically, [example] was one of graphene's different conditions.

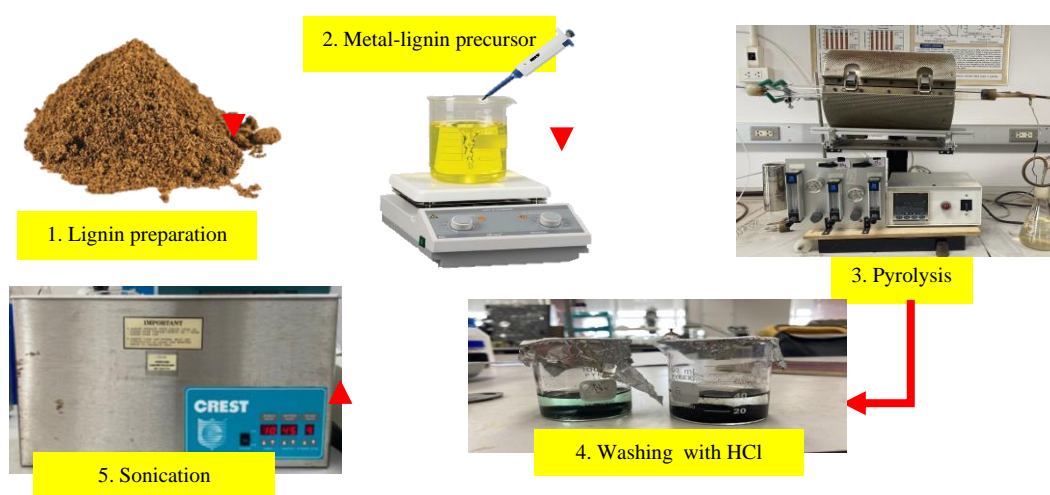


Fig. 1: Process flow chart of graphene synthesis

3.3 Characterization

The microstructure of the carbon materials was analyzed via the Raman spectra spectrometer (LabRAM HR Evolution, HORIBA). A He-Ne laser (532 nm) is the excitation source. Backscattered Raman



signals were collected through a microscope and holographic notch filters in the range of 3000 to 1000 cm^{-1} with a spectral resolution of 2 cm^{-1} . The specific area and porosities of samples were determined by Brunauer-Emmet-Teller (BET) analysis (Belsorp Mini II). SEM-EDS analysis (Hitachi SU5000) was performed to characterize the synthesized biobased graphene's structure and surface elemental compositions.

3.4 Electrochemical measurements

In order to prepare the electrode, synthesized graphene was blended with conductive carbon (Super P) and polyvinylidene fluoride (PVDF) at a weight ratio of 90:5:5 in an N-methyl-2-pyrrolidone (NMP) solvent. The slurry was coated with copper foil for use as a current collector. The electrodes were dried for 12 hours at 60 °C in an oven and then for 6 hours at 60 °C in a vacuum oven. The thickness of the coated slurry over copper foil was regulated to 20 μm , with a loading of 0.8–1.2 mg cm^{-2} . The counter electrode, made of pure lithium foil and a separator, was built into coin-cell batteries using an Ar-filled glove box. The electrolyte was prepared by dissolving LiPF_6 1 mol/L and fluoroethylene carbonate (FEC) additives at 6 vol% in a solution of ethylene carbonate and diethyl carbonate in a volume ratio of 1:1 (Phachwisoot, et al., 2021). Cyclic voltammetry (CV) tests were performed between 0 and 1 V using scan rates of 5–100 mV s^{-1} . Electrochemical impedance spectroscopy (EIS) measurements were conducted in the frequency range of 0.1–10,000 Hz. Galvanostatic charge–discharge (GCD) tests were performed at potentials ranging from 0 to 1 V and current densities of 0.1–20 A g^{-1} (Butcha, et al., 2023).

4. Results and Discussion

In a literature review, lignin was used as a carbon source to prepare biobased graphene. Seven sources of lignin, including commercial organosolv lignin (CL), empty fruit bunch lignin (EFBL), rubber wood lignin (RL), pine wood lignin (PL), eucalyptus lignin (EUL), bagasse lignin (BL), and extracted lignin (EL), were carried out to study the effect of lignin sources on the properties of synthesized graphene. The sources of lignin and the lignin extraction method were strongly related to the formation of graphene. The graphene product with parallel graphene sheet structures and a high surface area was obtained when using lignin derived from bagasse as the raw material. In this study, graphene was synthesized from lignin by catalytic pyrolysis. There were three sources of lignin used in this work: commercial organosolv lignin (CL), bagasse lignin from the Thai Roong Ruang Sugar Group (TL), and Mitr Phol (ML). It should be noted that TL and ML were obtained from sugarcane bagasse but obtained from different extraction procedures. Based on (Zhao, et al., 2020), the major ratio and holding time were metal: lignin (1:2.5) and 3 hours, respectively.

Firstly, the surface area and porosities of synthesized graphene are presented in Table 1. The surface area of synthesized graphene was within the range of 10–330 m^2/g depending on the lignin precursors. The surface areas of synthesized graphene from bagasse lignin (G-ML and G-TL) differ significantly, indicating that bagasse lignin from Thai Roong Ruang sugar is suitable for producing high surface area graphene. It is reasonable to deduce that the lignin sources and extraction process have a vital effect on the morphological properties of synthesized graphene. The synthesized graphene prepared from iron nitrate and nickel nitrate has a higher surface area because nickel and iron metal have higher activity with the cracking of C-H, C-O, and other bonding in biomass resources (Yan, et al., 2018).

Table 1: Surface area and porosities of synthesized graphene with different sources

Sample	Surface area (m^2/g)	Total pore volume (cm^3/g)
G-CL-Fe	10.93	0.04
G-CM-Ni	12.22	0.04
G-ML-Fe	53.01	0.07
G-TL-Fe	332.71	0.22
G-ML-Ni	10.40	0.03

[587]



Table 2 examines the surface area of synthesized graphene with different holding times and loading metal additives at the suggested ratio. The suitable time for the nickel additive is important for improving the surface area of graphene. Therefore, synthesized graphene is relatively higher when various holding times in synthesized graphene from nickel additive were 1 hour.

Table 2: Surface area and porosities of synthesized graphene with different holding times

Sample	Surface area (m ² /g)	Total pore volume (cm ³ /g)
G-TL-Fe	332.71	0.22
G-TL-Fe[H+1]	254.49	0.23
G-TL-Fe [H-1]	305.32	0.24
G-TL-Fe [H-2]	41.56	0.03
G-TL-Ni	125.46	0.14
G-TL-Ni [H+1]	98.47	0.12
G-TL-Ni [H-1]	171.01	0.16
G-TL-Ni [H-2]	244.80	0.24

Raman spectra of synthesized graphene were collected to examine the quality of graphene products, and the results are presented in Figure 2. The three primary peaks that were present in all the samples were the G peak (1580 cm⁻¹), the 2D peak (2670 cm⁻¹), and the D peak (1330 cm⁻¹). The former represents the vibration of sp²-hybrid carbon atoms in structural defects, whereas the latter represents sp²-bonded crystalline carbon. A standard indicator of the degree of graphitization is the intensity ratio of the D to G peak (I_D/I_G) (Mei, et al., 2021). The number of graphene layers is also positively correlated with the peak intensity ratio of the G peak to the 2D peak (I_G/I_{2D}). The significant surface area of graphene causes it to be unstable. The spontaneous aggregation of graphene will lead to its losing energy. The Raman 2D peak declined significantly due to the graphene powder becoming highly agglomerated by drying. (Dong, et al., 2020). The higher I_D/I_G and I_G/I_{2D} values demonstrate more defects in the samples. Synthesized graphene from TL lignin with nickel catalyst and increased holding time (G-TL-Ni [H+1]) has a strongly 2D peak, which indicates a few-layer graphene sheet.

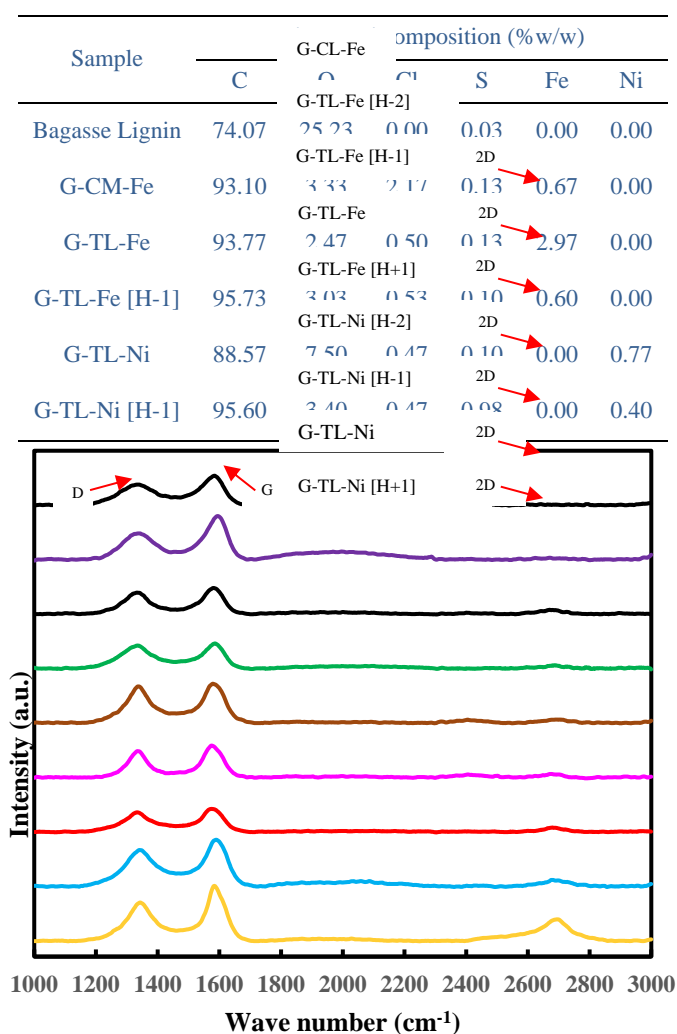


Fig. 2: Raman spectra of synthesized graphene

SEM-EDS analysis was used to examine the structure and surface elemental compositions of the produced graphene. Table 3 presents the elemental compositions of synthesized graphene. Overall, there is no notable difference in the elemental compositions of the other synthesized graphene. Furthermore, all graphene samples show low impurities (Fe, Ni, S, and Cl, <3%), suggesting the successful removal of the metal catalyst.

**Table 3:** Elemental compositions of synthesized graphene.

Figure 3 shows that many of the structures of synthesized graphene are irregular condensation structures, as shown in G-TL-Fe. The size and volume of porosity are readily visible, corresponding to a high surface area. In contrast, the nickel precursor in G-TL-Ni makes the surface glossy and smooth.

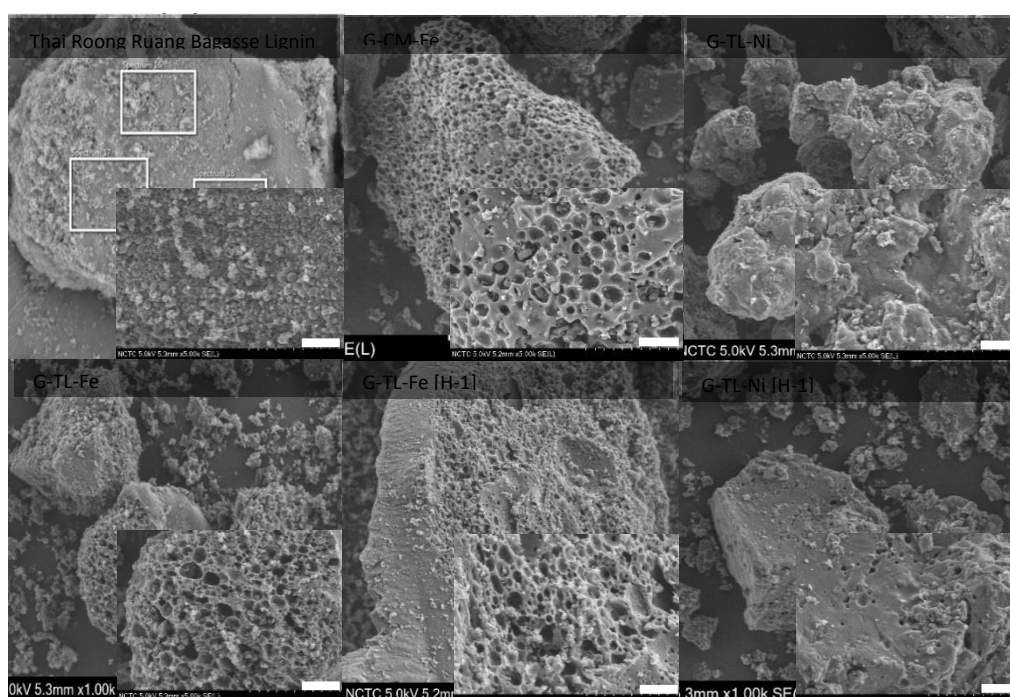
**Fig. 3:** SEM images of synthesized graphene

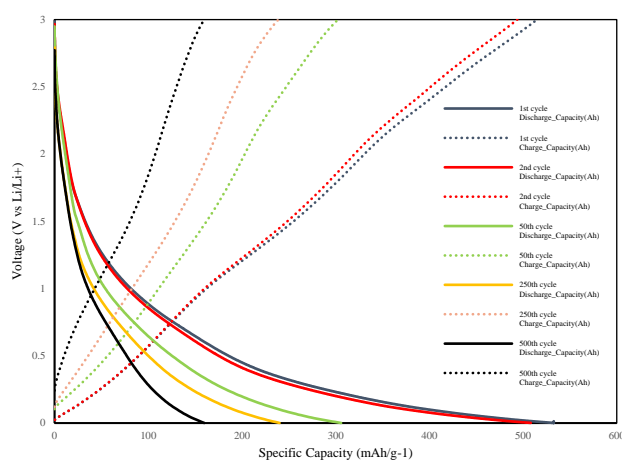
Figure 4(a) presents the charge/discharge curves of synthetic graphene used as an anode in Lithium-ion battery applications at a current density of 100 mA g^{-1} . The 1st and 2nd cycles had discharge capacities of 532 and 508 mA g^{-1} and charge capacities of 514 and 493 mA g^{-1} . The battery coulombic efficiency can be correlated to 96% and 97%, respectively. It should be mentioned that the second specific discharge capacity is 1.4 times greater than the theoretical value of 372 mA g^{-1} of graphite. The considerable capacity loss in the 1st cycle is caused by the formation of the solid electrolyte interphase (SEI) film and the irreversible lithium storage in disordered carbon structures (Butcha, et al., 2023). Figure 4(b) compares the specific capacities of synthesized graphene and commercial graphite. The activation procedures for the first three cycles were generally carried out at a current rate of 100 mA g^{-1} , whereas the following cycles were carried out at a current rate of 1 Ag^{-1} . On the 100th cycle, the synthesized graphene had a discharge capacity of 315 mA g^{-1} , which was 2.2 times greater than that of commercial graphite. The cycling capability of the produced graphene was tested at a current density of 1 Ag^{-1} . Figure 5 showed good cyclability after 300 cycles, with discharge capacity, charge capacity, and coulombic efficiency of 213 mA g^{-1} , 212 mA g^{-1} , and 99%,

[590]



respectively.

(a)



(b)

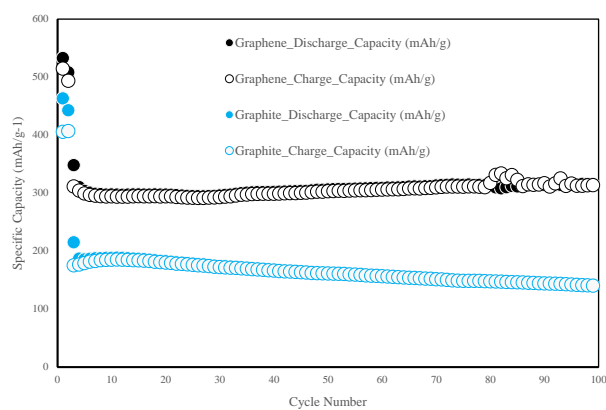


Fig. 4: Electrochemical performance of synthesized graphene as an anode material in lithium-ion batteries: (a) discharge/charge curves at 100 mA g^{-1} ; (b) cycling performance of the synthesized graphene compared with commercial graphite at a scan rate of 1 A g^{-1}

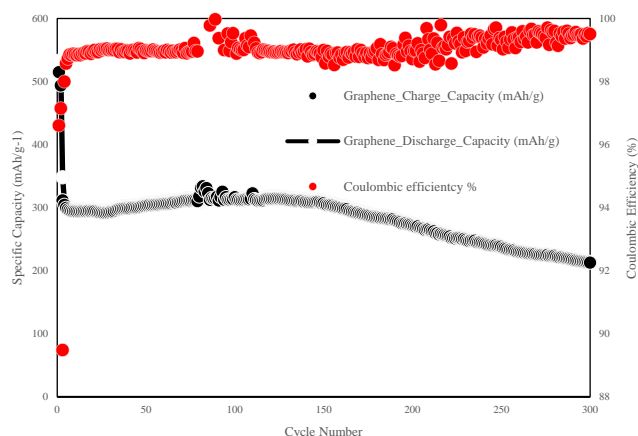


Fig. 5: Cycling performance of synthesized graphene as an anode material in lithium-ion batteries at a scan rate of 1 A g^{-1}

5. Conclusion

In this work, lignin was used as a carbon source to prepare biobased graphene. Three sources of lignin, including commercial organosolv lignin (CL), Thai Roong Ruang sugarcane bagasse, and Mitr Phol sugarcane bagasse, were carried out to study the effect of lignin sources on the properties of graphene products. The suitable ratios and holding times in the method are strongly related to the surface area of graphene. The synthesized graphene with parallel graphene sheet structures and a high surface area was obtained when using lignin derived from Thai Roong Ruang bagasse as the raw material. According to synthesized graphene, iron additive have a higher surface area than nickel additives. Finally, at a current rate of 100 mA g^{-1} , the synthesized graphene used in the lithium-ion battery anode demonstrates a good specific capacity of 532 mA g^{-1} , which is 1.4 times higher than that of commercial graphite. After testing for up to 300th cycles at a current density of 1 A g^{-1} , the synthesized graphene likewise demonstrated high performance, with a coulombic efficiency of 99%.

6. References

- Butcha, S., Rajruthong, C., Sattayarat, V., Youngjan, S., Nakajima, H., Supruangnet, R., ... & Khemthong, P. (2023). Sustainable production of multifunctional hierarchical carbon from weed water hyacinth: assessment for lithium-ion battery and supercapacitor. *Journal of Energy Storage*, 72, 108578.
- Dong, H., Li, M., Jin, Y., Wu, Y., Huang, C., & Yang, J. (2020). Preparation of Graphene-Like porous carbons with enhanced thermal conductivities from lignin nano-particles by combining hydrothermal carbonization and pyrolysis. *Frontiers in Energy Research*, 8. <https://doi.org/10.3389/fenrg.2020.00148>
- Phachwisoot, G., Nakason, K., Chanthad, C., Khemthong, P., Kraithong, W., Youngjan, S., & Panyapinyopol, B. (2021b). Sequential Production of Levulinic Acid and Supercapacitor Electrode Materials from Cassava Rhizome through an Integrated Biorefinery Process. *ACS Sustainable Chemistry & Engineering*, 9(23), 7824–7836. <https://doi.org/10.1021/acssuschemeng.1c01335>
- Ishii, T., Mori, M., Hisayasu, S., Tamura, R., Ikuta, Y., Fujishiro, F., Ozaki, J., Itabashi, H., & Mori, M. (2021). Direct conversion of lignin to high-quality graphene-based materials via catalytic carbonization. *RSC Advances*, 11(31), 18702–18707. <https://doi.org/10.1039/d1ra02491d>

[592]



- Jung, H., Lee, J., Han, H., Jung, J., Eom, K., & Lee, J. (2022). Lignin-Based Materials for Sustainable Rechargeable Batteries. *Polymers*, 14(4), 673. <https://doi.org/10.3390/polym14040673>
- Kai, D., Tan, M. J., Chee, P. L., Chua, Y. K., Yap, Y. L., & Loh, X. J. (2016). Towards lignin-based functional materials in a sustainable world. *Green Chemistry*, 18(5), 1175–1200. <https://doi.org/10.1039/c5gc02616d>
- Lee, C., Wei, X., Kysar, J. W., & Hone, J. (2008). Measurement of the elastic properties and intrinsic strength of monolayer graphene. *Science (New York, N.Y.)*, 321(5887), 385–388. <https://doi.org/10.1126/science.1157996>
- Liengprayoon, S., Suphamitmongkol, W., Jantarasunthorn, S., Rungjang, W., Sunthornvarabhas, J., & Tanthana, J. (2019). Investigation of the potential for utilization of sugarcane bagasse lignin for carbon fiber production: Thailand case study. *SN Applied Sciences (Print)*, 1(10). <https://doi.org/10.1007/s42452-019-1205-x>
- Liu, F., Chen, Y., & Gao, J. (2017). Preparation and Characterization of Biobased Graphene from Kraft Lignin. *Bioresources*, 12(3). <https://doi.org/10.15376/biores.12.3.6545-6557>
- Liu, H., Xu, T., Liu, K., Zhang, M., Liu, W., Li, H., . . . Si, C. (2021). Lignin-based electrodes for energy storage application. *Industrial Crops and Products*, 165, 113425. <https://doi.org/10.1016/j.indcrop.2021.113425>
- Lu, X., & Gu, X. (2022). A review on lignin pyrolysis: pyrolytic behavior, mechanism, and relevant upgrading for improving process efficiency. *Biotechnology for Biofuels and Bioproducts*, 15(1), 106. <https://doi.org/10.1186/s13068-022-02203-0>
- Mandlekar, N., Cayla, A., Rault, F., Giraud, S., Salaün, F., Malucelli, G., & Guan, J. (2018). An overview on the use of lignin and its derivatives in fire retardant polymer systems. In *InTech eBooks*. <https://doi.org/10.5772/intechopen.72963>
- Mei, S., Liu, Y., Fu, J., Guo, S., Deng, J., Peng, X., Zhang, X., Gao, B., Huo, K., & Chu, P. K. (2021). Waste-glass-derived silicon/CNTs composite with strong Si-C covalent bonding for advanced anode materials in lithium-ion batteries. *Applied Surface Science*, 563, 150280. <https://doi.org/10.1016/j.apsusc.2021.150280>
- Okhay, O., & Tkach, A. (2021). Graphene/Reduced Graphene Oxide-Carbon Nanotubes Composite Electrodes: From Capacitive to Battery-Type Behaviour. *Nanomaterials*, 11(5), 1240. <https://doi.org/10.3390/nano11051240>
- Phachwisoot, G., Nakason, K., Chanthad, C., Khemthong, P., Kraithong, W., Youngjan, S., & Panyapinyopol, B. (2021). Sequential Production of Levulinic Acid and Supercapacitor Electrode Materials from Cassava Rhizome through an Integrated Biorefinery Process. *ACS Sustainable Chemistry & Engineering*, 9(23), 7824–7836. <https://doi.org/10.1021/acssuschemeng.1c01335>
- Pongchaiphol, S., Preechakun, T., Raita, M., Champreda, V., & Laosiripojana, N. (2021). Characterization of Cellulose–Chitosan-Based Materials from Different Lignocellulosic Residues Prepared by the



- Ethanosolv Process and Bleaching Treatment with Hydrogen Peroxide. *ACS Omega*, 6(35), 22791-22802. <https://doi.org/10.1021/acsomega.1c03141>
- Pongchaiphol, S., Suriyachai, N., Hararak, B., Raita, M., Laosiripojana, N., & Champreda, V. (2022). Physicochemical characteristics of organosolv lignins from different lignocellulosic agricultural wastes. *International Journal of Biological Macromolecules*, 216, 710-727. <https://doi.org/10.1016/j.ijbiomac.2022.07.007>
- Poorna, A., Saravanathamizhan, R., & Balasubramanian, N. (2020). Graphene and graphene-like structure from biomass for Electrochemical Energy Storage application- A Review. *Electrochemical Science Advances*, 1(3). <https://doi.org/10.1002/elsa.202000028>
- Shams, S. S., Zhang, L. S., Hu, R., Zhang, R., & Zhu, J. (2015). Synthesis of graphene from biomass: A green chemistry approach. *Materials Letters*, 161, 476-479. <https://doi.org/10.1016/j.matlet.2015.09.022>
- Thermo Fisher Scientific, i. (2019). *Characterizing graphene with Raman spectroscopy*. (A. 07/19M, Ed.)
- Yan, Q., Li, J., Zhang, X., Hassan, E. B., Wang, C., Zhang, J., & Cai, Z. (2018). Catalytic graphitization of kraft lignin to graphene-based structures with four different transitional metals. *Journal of Nanoparticle Research*, 20, 1-20.
- Yan, Q., Li, J., Zhang, X., Hassan, E. B., Wang, C., Zhang, J., & Cai, Z. (2018). Catalytic graphitization of kraft lignin to graphene-based structures with four different transitional metals. *Journal of Nanoparticle Research*, 20(9). <https://doi.org/10.1007/s11051-018-4317-0>
- Zhang, W., Qiu, X., Wang, C., Zhong, L., Fu, F., Zhu, J., Zejie, Z., Qin, Y., Yang, D., & Xu, C. (2022). Lignin derived carbon materials: current status and future trends. *Carbon Research*, 1(1). <https://doi.org/10.1007/s44246-022-00009-1>
- Zhao, W., Tan, P., Zhang, J., & Liu, J. (2010). Charge transfer and optical phonon mixing in few-layer graphene chemically doped. *PHYSICAL REVIEW B*, 82(24), 245423.
- Zhao, Y., Wen, M., He, C., Liu, C., Li, Z., & Liu, Y. (2020). Preparation of graphene by catalytic pyrolysis of lignin and its electrochemical properties. *Materials Letters*, 274, 128047. <https://doi.org/10.1016/j.matlet.2020.128047>
- Zhu, J., Duan, R., Zhang, S., Jiang, N., Zhang, Y., & Zhu, J. (2014). The application of graphene in lithium ion battery electrode materials. *SpringerPlus (Cham)*, 3(1). <https://doi.org/10.1186/2193-1801-3-585>
- Zhu, J., Yan, C., Zhang, X., Yang, C., Jiang, M., & Xiangwu, Z. (2020). A sustainable platform of lignin: From bioresources to materials and their applications in rechargeable batteries and supercapacitors. *Progress in Energy and Combustion Science*, 76, 100788. <https://doi.org/10.1016/j.pecs.2019.100788>